

Supplementary Information for

Ultrahigh energy storage density, high efficiency and superior thermal stability in
 $\text{Bi}_{0.5}\text{Na}_{0.5}\text{TiO}_3$ -based relaxor ferroelectric ceramics *via* constructing multiphase
structures

Yi-Ning Huang¹, Ji Zhang^{1,*}, Jiajia Wang¹, Jing Wang^{2,*}, Yaojin Wang^{1,*}

¹ School of Materials Science and Engineering, Nanjing University of Science &
Technology, Nanjing 210094, China

² State Key Laboratory of Mechanics and Control of Mechanical Structures, College of
Aerospace Engineering, Nanjing University of Aeronautics and Astronautics, Nanjing
210016, China

*Corresponding authors: jizhang@njust.edu.cn; wang-jing@nuaa.edu.cn;
yjwang@njust.edu.cn

Experimental Procedure

$(1-x)\text{Bi}_{0.5}\text{Na}_{0.5}\text{TiO}_3-x\text{Ba}_{0.7}\text{Sr}_{0.3}\text{Zr}_{0.8}\text{Sn}_{0.2}\text{O}_3$ ceramics with $x = 0, 0.10, 0.15, 0.20, 0.25$ were fabricated by solid-state reaction. High purity oxides and carbonate of Bi_2O_3 (99.9%), Na_2CO_3 (99.99%), TiO_2 (99%), BaCO_3 (99.95%), SrCO_3 (99.95%), ZrO_2 (99%), SnO_2 (99.5%, all from Aladdin) were selected as starting materials and weighted according to designed composition. Then, all the weighted powders were mixed with ethanol and with ZrO_2 balls in nylon tank by a planetary ball mill. Afterwards, the slurry was dried, and calcined at 800°C . Subsequently, the calcined powders were ball-milled again, dried and mixed with polyvinyl butyral as binder, then pressed into disks with thickness of ~ 1 mm and diameter of ~ 10 mm under 10 MPa. The binder was removed at 600°C with increasing rate of $2^\circ\text{C}/\text{min}$. Eventually, the green disks were pressed again under 120 MPa by cold isostatic pressing and sintered at 1150°C . The increasing and decreasing rate for temperature variety were both $5^\circ\text{C}/\text{min}$. During sintering, the samples were embedded in powders with the same composition to suppress the volatilization of Bi and Na.

Crystalline structure of ceramics was detected by X-ray diffraction (XRD, PANalytical), and the FULLPROF software was adopted to perform the structural refinement. The microstructure was confirmed by field-emission scanning electron microscopy (SEM, Zeiss Ultra-55). For dielectric property measurements, the surfaces of the polished disks were covered with silver paste and fired at 550°C for 30 min. The temperature-dependent permittivity (ϵ_r) and loss ($\tan\delta$) were measured using an LCR meter (Agilent E4980A, Santa Clara, CA) at various frequencies. The specific electric

breakdown strength of each sample was collected by a voltage-withstand test device (Trek 610D, PolyK Technologies), and the polarization-electric field (P - E) curves were tested by a ferroelectric analyzer (Radiant Technologies). The charge-discharge property was characterized by a specially RLC load circuit (PK-CPR1701, PolyK Technologies). For P - E loops and direct charge/discharge, the sample thickness and electrode area are 0.1 mm and 0.785 mm² (1 mm in diameter).

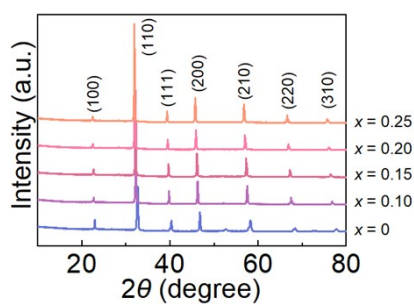


Fig. S1 XRD patterns of $(1-x)\text{BNT}-x\text{BSZS}$ ceramics.

Table S1 The Refined structural parameters of (1-x)BNT-xBSZS ceramics.

	$x = 0$	$x = 0.10$		$x = 0.15$		$x = 0.20$		$x = 0.25$	
Space group	<i>R3c</i>	<i>R3c</i> (84%)	<i>P4bm</i> (16%)	<i>R3c</i> (67%)	<i>P4bm</i> (33%)	<i>R3c</i> (56%)	<i>P4bm</i> (44%)	<i>R3c</i> (32%)	<i>P4bm</i> (68%)
a (Å)	5.4816	5.5465	5.5503	5.5706	5.5685	5.5940	5.5935	5.6171	5.6155
b (Å)	5.4816	5.5465	5.5503	5.5706	5.5685	5.5940	5.5934	5.6171	5.6155
c (Å)	13.5342	13.5834	3.9230	13.6411	3.9393	13.7022	3.9594	13.7536	3.9745
α	90°	90°	90°	90°	90°	90°	90°	90°	90°
β	90°	90°	90°	90°	90°	90°	90°	90°	90°
γ	120°	120°	90°	120°	90°	120°	90°	120°	90°
Cell volume	352.195	361.885	120.853	366.593	122.148	371.335	123.875	375.809	125.332
R_{wp}	6.56	8.42		7.92		7.90		8.30	
R_p	4.83	4.75		4.65		4.68		4.64	
χ^2	5.25	9.25		7.91		7.15		8.94	

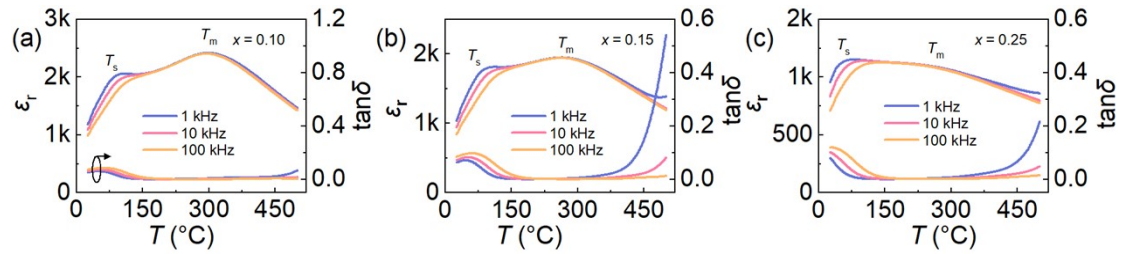


Fig. S2 Temperature-dependent permittivity (ϵ_r) and loss ($\tan\delta$) of (a) $x = 0.10$, (b) $x = 0.15$, (c) $x = 0.25$.

Table S2 β values of BNT-BSZS ceramics.

Composition	$x = 0$	$x = 0.10$	$x = 0.15$	$x = 0.20$	$x = 0.25$
β	18.1	13.7	8.5	12.7	10.1

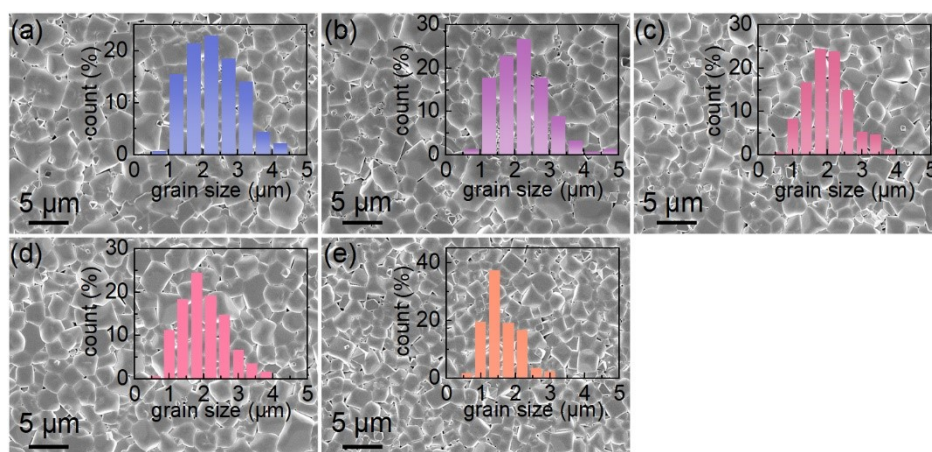


Fig. S3 SEM morphologies of BNT-BSZS ceramics and corresponding grain size distribution: (a) $x = 0$, (b) $x = 0.10$, (c) $x = 0.15$, (d) $x = 0.20$, (e) $x = 0.25$.

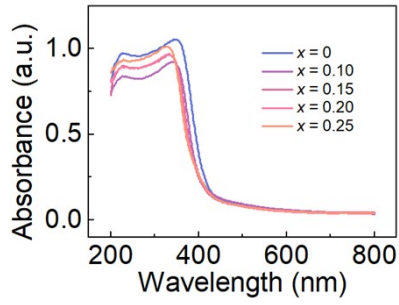


Fig. S4 UV-vis absorption spectrum of BNT-BSZS ceramics.

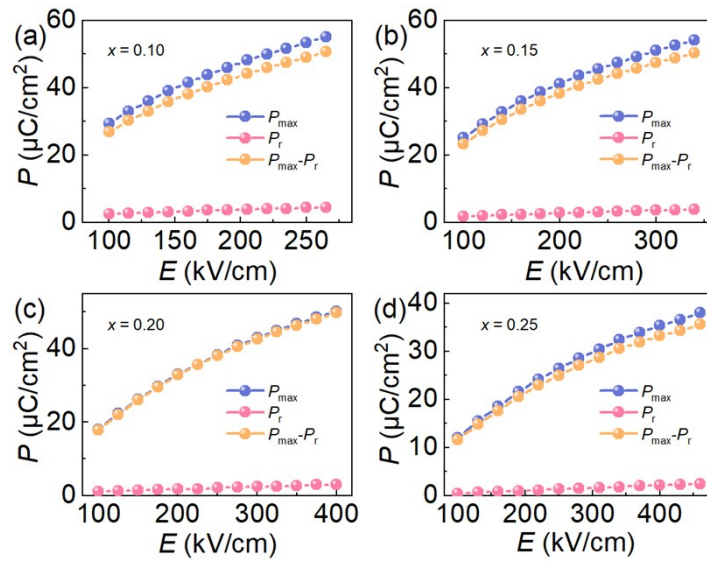


Fig. S5 Electric field dependent P_{\max} , P_r and $P_{\max}-P_r$ of (a) $x = 0.10$, (b) $x = 0.15$, (c) $x = 0.20$, (d) $x = 0.25$,

Table S3 Comparison of energy storage properties between this work and recently reported BNT-based ceramics.

Compositions	E (kV/cm)	W_{rec} (J/cm ³)	η (%)	Reference
$x = 0.10$	265	4.9	82	This work
$x = 0.15$	340	6.3	87.5	This work
$x = 0.20$	400	7.4	88.7	This work
$x = 0.25$	460	6.6	90.2	This work
0.62Na _{0.5} Bi _{0.5} TiO ₃ -0.3Sr _{0.7} Bi _{0.2} TiO ₃ - 0.08BiMg _{2/3} Nb _{1/3} O ₃	470	7.5	92	7
0.90(Bi _{0.5} Na _{0.5}) _{0.65} Sr _{0.35} TiO ₃ - 0.10Bi(Mg _{0.5} Zr _{0.5})O ₃	522	8.46	85.9	9
0.55Bi _{0.5} Na _{0.5} TiO ₃ -0.45Sr _{0.7} La _{0.2} TiO ₃	338	4.14	92.2	13
0.8(0.95Bi _{0.5} Na _{0.5} TiO ₃ -0.05SrZrO ₃)- 0.2NaNbO ₃	350	5.55	85	23
0.85(Bi _{0.5} Na _{0.5}) _{0.7} Sr _{0.3} TiO ₃ - 0.15Bi(Mg _{0.5} Sn _{0.5})O ₃	280	3.76	78.8	26
0.80Bi _{0.5} Na _{0.5} TiO ₃ -0.20SrNb _{0.5} Al _{0.5} O ₃	520	6.64	96.5	29
0.84Bi _{0.5} Na _{0.5} TiO ₃ -0.16KNbO ₃	320	5.2	88	30
0.78(Bi _{0.5} Na _{0.5})TiO ₃ -0.22NaNbO ₃	390	7.02	85	31
0.7(0.85Bi _{0.5} Na _{0.5} TiO ₃ -0.15NaNbO ₃)- 0.3(Sr _{1.05} Bi _{0.3})ScO ₃	540	7.3	80	32
0.90(Na _{0.5} Bi _{0.5}) _{0.7} Sr _{0.3} TiO ₃ - 0.10Bi(Ni _{0.5} Sn _{0.5})O ₃	270	4.18	83.64	33
0.86(Na _{0.5} Bi _{0.5}) _{0.6} Sr _{0.4} TiO ₃ - 0.14Sr _{0.7} La _{0.2} ZrO ₃	322	3.45	90.1	34
0.85Na _{0.5} Bi _{0.5} TiO ₃ -0.15CaZr _{0.5} Ti _{0.5} O ₃	297.7	4.37	81.4	35
0.5Na _{0.5} Bi _{0.5} TiO ₃ -0.5Sr _{0.85} Sm _{0.1} TiO ₃	422	5.02	90	36
0.6Bi _{0.5} Na _{0.5} TiO ₃ -0.4Sr _{0.7} Sm _{0.2} TiO ₃	260	3.52	84.2	37
0.86(0.93Na _{1/2} Bi _{1/2} TiO ₃ -0.07BaTiO ₃)- 0.14K _{1/2} Bi _{1/2} (Zn _{1/3} Nb _{2/3})O ₃	290	5.1	80	38
0.45Na _{0.5} Bi _{0.5} TiO ₃ - 0.55Sr _{0.7} Bi _{0.2} TiO ₃ /6wt%AlN	360	5.53	90	39
0.6[0.955(Bi _{0.5} Na _{0.5})TiO ₃ - 0.045Ba(Al _{0.5} Ta _{0.5})O ₃]-0.4CaTiO ₃	440	5.81	97.8	40
0.7Na _{0.5} Bi _{0.5} TiO ₃ - 0.3NaNbO ₃ /7wt%CaZr _{0.5} Ti _{0.5} O ₃	410	4.93	93.3	41
0.65Bi _{0.5} Na _{0.4} K _{0.1} TiO ₃ -0.35[2/3SrTiO ₃ - 1/3Bi(Mg _{2/3} Nb _{1/3})O ₃]	290	4.43	86	42
0.75Bi _{0.58} Na _{0.42} TiO ₃ -0.25SrTiO ₃	535	5.63	94	43

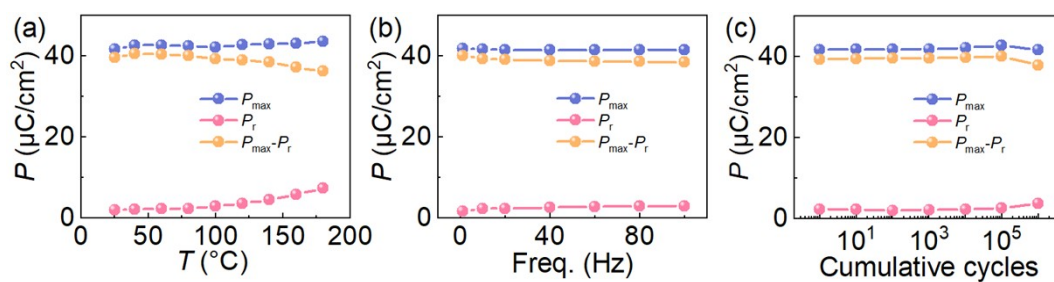


Fig. S6 Evolution of P_{\max} , P_r and $P_{\max} - P_r$ of $x = 0.2$ under different temperatures, frequencies and cycling numbers.